

“New Cathode Materials for Intermediate Temperature Solid Oxide Fuel Cells”
Quarterly Report for 4/1/2004 to 6/30/2004

DE-FC26-03NT41960

July 23, 2004

Allan J Jacobson
Center for Materials Chemistry
University of Houston
Houston, Texas 77204-5003

“This report was prepared as an account of work sponsored by an agency of the United States Government. Neither the United States Government nor any agency thereof, nor any of their employees, makes any warranty, express or implied, or assumes any legal liability or responsibility for the accuracy, completeness, or usefulness of any information, apparatus, product, or process disclosed, or represents that its use would not infringe privately owned rights. Reference herein to any specific commercial product, process, or service by trade name, trademark, manufacturer, or otherwise does not necessarily constitute or imply its endorsement, recommendation, or favoring by the United States Government or any agency thereof. The views and opinions of authors expressed herein do not necessarily state or reflect those of the United States Government or any agency thereof.”

Abstract

Operation of SOFCs at intermediate temperatures (500 – 800 °C) requires new combinations of electrolyte and electrode materials that will provide both rapid ion transport across the electrolyte and electrode - electrolyte interfaces and efficient electrocatalysis of the oxygen reduction and fuel oxidation reactions. This project concentrates on materials and issues associated with cathode performance that are known to become limiting factors as the operating temperature is reduced.

The specific objectives of the proposed research are to develop cathode materials that meet the electrode performance targets of 1.0 W/cm² at 0.7 V in combination with YSZ at 700 °C and with GDC, LSGM or bismuth oxide based electrolytes at 600 °C. The performance targets imply an area specific resistance of ~0.5 Ωcm² for the total cell. The research strategy is to investigate both established classes of materials and new candidates as cathodes, to determine fundamental performance parameters such as bulk diffusion, surface reactivity and interfacial transfer, and to couple these parameters to performance in single cell tests.

The initial choices for study are perovskite oxides based on Sr substituted LaFeO₃, where significant data in single cell tests exists at PNNL for cathodes on both YSZ and CSO/YSZ, and Ln₂NiO₄ compositions. A key component of the research strategy is to evaluate for each cathode material composition, the key performance parameters, including ionic and electronic conductivity, surface exchange rates, stability with respect to the specific electrolyte choice, and thermal expansion coefficients. Results on electrical conductivity relaxation measurements on additional compositions in the La₂NiO_{4+x} and Pr₂NiO_{4+x} series are presented in this report. Studies of the inter-diffusion of amorphous SrFeO_{3-x} and LaFeO_{3-x} bilayer films prepared by pulsed laser deposition are described. Such studies are a preliminary to the combinatorial synthesis approach discussed in previous reports.

Table of Contents

1.	List of Graphical Materials	3
2.	Introduction	4
3.	Executive Summary	4
4.	Experimental	4
4.1	Characterization of K1 Compositions $\text{La}_x\text{Pr}_{2-x}\text{NiO}_{4+x}$ ($x = 1.9, 1.2, 1.0$).	4
4.2	DC conductivity Measurements of $\text{La}_x\text{Pr}_{2-x}\text{NiO}_{4+\delta}$ ($x = 1.9, 1.2, 1.0$)	5
4.3	Electrical Conductivity Relaxation Measurements	6
5.	Combinatorial Approach to Measurement of Transport Parameters.	7
5.1	Interdiffusion of Amorphous Bilayer Films of LaFeO_3 and $\text{SrFeO}_{2.5}$.	8
5.2	Surface Analysis of LaFeO_3 / SrFeO_3 on LAO	9
6	Conclusions	10
7	References	10
8	List of Acronyms and Abbreviations	11
9	Milestones	11

1. List of Graphical Materials

Figure 1. Cell parameters a , b and c (Å) versus x in $\text{La}_x\text{Pr}_{2-x}\text{NiO}_{4+d}$
Figure 2. Conductivity data for $\text{La}_x\text{Pr}_{2-x}\text{NiO}_{4+d}$ ($x = 0.1, 0.8$ and 1) at 10% and 1% $p\text{O}_2$
Figure 3. Figure 3. Comparison of the DC conductivities for $\text{La}_{2-x}\text{Pr}_x\text{NiO}_{4+d}$ vs. temperature and vs composition at $100/T = 2.0$.
Figure 4. Figure 4 Values of D_{chem} (left) and k_{chem} (right) of $\text{La}_x\text{Pr}_{2-x}\text{NiO}_{4+d}$ ($x = 1.9, 1.2$ and 1)
Figure 5. Schematic of the Approach to Make Multiple Compositions on One Substrate.
Figure 6. XRD spectra of annealed thin films on LAO substrate, a) $\text{SrFeO}_3/\text{LaFeO}_3$ b) $\text{LaFeO}_3/\text{SrFeO}_3$, after heated in O_2 at $380\text{ }^\circ\text{C}$ for 110 h and followed by $715\text{ }^\circ\text{C}$ for 8 h .
Figure 7. Ga^+ SIMS depth profile of LaFeO_3 on SrFeO_3 on a LAO substrate.

2. Introduction

The objectives of the project are to discover new oxide cathode materials that meet a performance target of 1.0 W/cm^2 at 0.7 V in combination with YSZ at $700 \text{ }^\circ\text{C}$ and with CGO, LSGM electrolytes at $600 \text{ }^\circ\text{C}$. An ancillary objective of the project is to increase fundamental understanding of the intrinsic transport properties of mixed electronic ionic conducting oxides and oxide-oxide interfaces that can be used to accelerate further progress in the development of cost effective high performance solid oxide fuel cells. In Phase I, we are measuring the surface exchange rates, diffusion coefficients and interfacial transport for an initial set of perovskite related oxide materials. In Phase II we will synthesize and characterize new cathode materials and measure their kinetic parameters. The thermal and chemical compatibility with different electrolytes will be determined. Based on the results, a subset of the best materials will be selected for single cell tests. The phase III objectives are to evaluate the performance of the best materials identified in Phase I and II. The optimum electrode composition and microstructure will be determined and the longer term performance characteristics evaluated.

3. Executive Summary

The project began on October 1, 2003 and this is the third quarterly report. In the third period, we have prepared and characterized single phase samples of $\text{La}_x\text{Pr}_{2-x}\text{NiO}_{4+x}$ ($x = 1.9, 1.2$ and 1.0) for comparison with the end members $\text{La}_2\text{NiO}_{4+x}$ and $\text{Pr}_2\text{NiO}_{4+x}$.¹⁻⁹ We have measured the dc conductivities as a function of pO_2 in several oxygen partial pressures. We have made preliminary electrical conductivity relaxation measurements as function of temperature for several different pO_2 switches. Thermogravimetric analysis measurements are in progress to provide the stoichiometry data needed to extract the oxygen ion diffusion coefficients and the surface exchange coefficients for comparison with previous measurements. We have also started to prepare thin oxide films by pulsed laser deposition for study of transport kinetics. We have decided to adopt a combinatorial approach, initially with the $\text{LaFeO}_3 - \text{SrFeO}_{2.5}$ system to determine synthesis and evaluation conditions. Amorphous two layer thin films of LaFeO_3 and $\text{SrFeO}_{2.5}$ have been prepared by PLD in amorphous form and their interdiffusion at $400 \text{ }^\circ\text{C}$ investigated. Further work is necessary to find the optimum conditions and to reduce surface roughness that occurs during annealing.

4. Experimental

4.1 Characterization of K1 Compositions $\text{La}_x\text{Pr}_{2-x}\text{NiO}_{4+x}$ ($x = 1.9, 1.2, 1.0$).

The syntheses and compositional characterization of additional K1 compositions in the series $\text{Ln}_2\text{NiO}_{4+x}$, $\text{Ln} = \text{La, Pr}$, have been prepared using the synthesis method described in the previous report. The phase purity and lattice parameters were determined by powder X-ray diffraction.

The cell parameters for a series of compositions $\text{La}_x\text{Pr}_{2-x}\text{NiO}_{4+d}$ ($x = 2, 1.9, 1.2, 1.0$ and 0) are shown in Figure 1. Substitution of praseodymium for lanthanum leads to an overall

decrease of the cell volume consistent with the respective ionic radii. $\text{La}_2\text{NiO}_{4+\delta}$ and $\text{Pr}_2\text{NiO}_{4+\delta}$ are isostructural, but the ionic radius of La^{3+} ($r = 1.16 \text{ \AA}$) is a little larger than that of Pr^{3+} ($r = 1.126 \text{ \AA}$). The change in the non-stoichiometry (δ) also needs to be taken into account; δ in $\text{La}_2\text{NiO}_{4+\delta}$ is smaller than that in $\text{Pr}_2\text{NiO}_{4+\delta}$ but the data for the other compositions is not yet available. The abrupt change of cell parameters between $x = 1 \sim 1.2$ may reflect changes in oxygen stoichiometry but further measurements are needed to clarify this point.

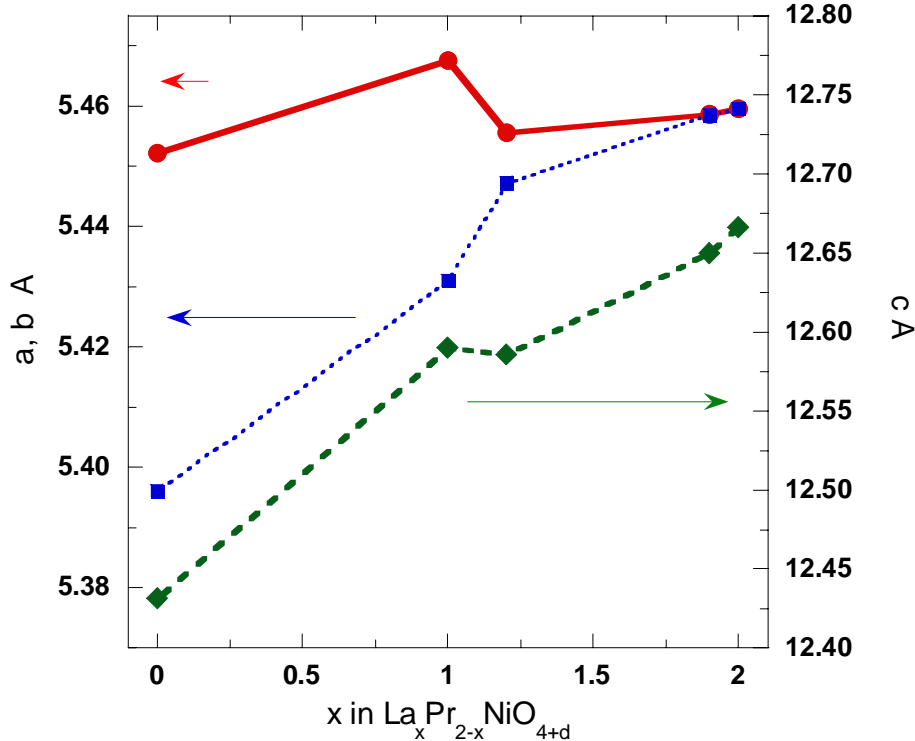


Figure 1 Cell parameters a, b and c (\AA) versus x in $\text{La}_x\text{Pr}_{2-x}\text{NiO}_{4+\delta}$

4.2 DC conductivity Measurements of $\text{La}_x\text{Pr}_{2-x}\text{NiO}_{4+\delta}$ ($x = 1.9, 1.2$ and 1.0)

DC conductivity measurements using the 4 probe method were made using rectangular shaped bars for $\text{La}_{1.9}\text{Pr}_{0.1}\text{NiO}_{4+\delta}$ ($12.6 \times 1.6 \times 2.0 \text{ mm}$), $\text{La}_{1.2}\text{Pr}_{0.8}\text{NiO}_{4+\delta}$ ($12.9 \times 1.7 \times 2.2 \text{ mm}$), and $\text{LaPrNiO}_{4+\delta}$ ($12 \times 2.1 \times 1.9 \text{ mm}$). Each composition has a high conductivity ($\sim 100 \text{ S/cm}$) in 0.1 and 0.01 pO_2 atm (see Figure 2) and a different roll over temperature where oxygen loss offsets the effect of increasing temperature (315 K for $\text{LaPrNiO}_{4+\delta}$, 450 K for $\text{La}_{1.2}\text{Pr}_{0.8}\text{NiO}_{4+\delta}$, and 320 K for $\text{La}_{1.9}\text{Pr}_{0.1}\text{NiO}_{4+\delta}$, respectively). The results for all compositions measured in 1% oxygen are shown in Figure 3. With increasing substitution of Pr into La, the conductivity increases after an initial large decrease from the value for pure $\text{La}_2\text{NiO}_{4+\delta}$. Some evidence for a correlation with changes in the cell constants can be seen in Figure 3(right) but additional measurements are needed to confirm this

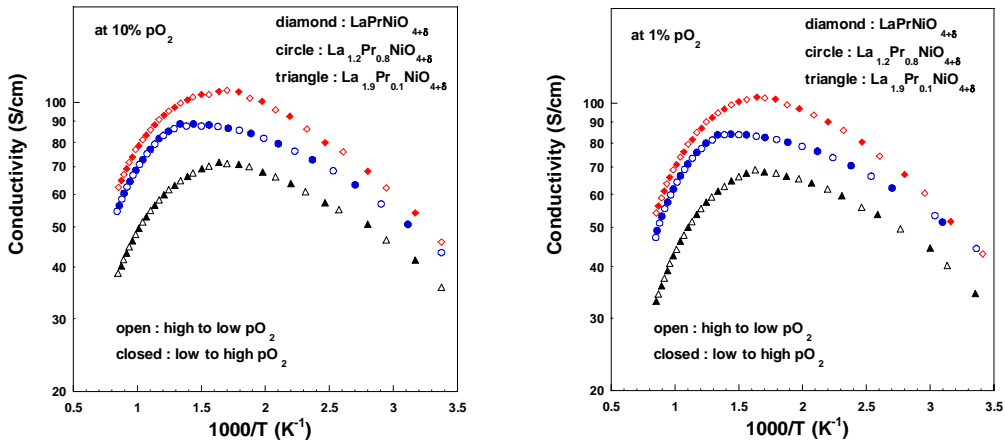


Figure 2 Conductivity data for $\text{La}_x\text{Pr}_{2-x}\text{NiO}_{4+d}$ ($x = 1.9, 1.2$ and 1) at 10% and 1% pO_2

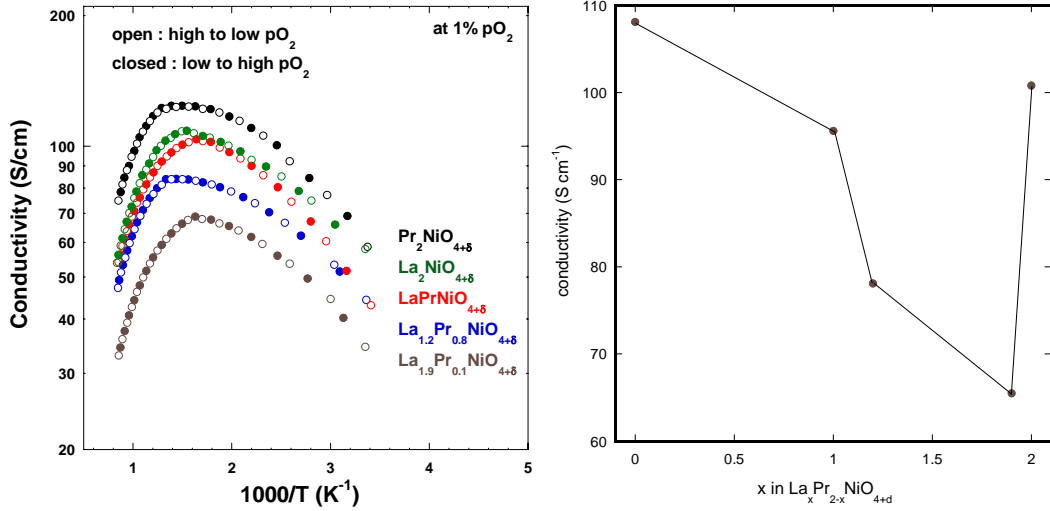


Figure 3. Comparison of the DC conductivities for $\text{La}_x\text{Pr}_{2-x}\text{NiO}_{4+d}$ vs. temperature and vs. composition at $1000/T = 2.0$.

4.3 Electrical Conductivity Relaxation Measurements

Electrical conductivity relaxation measurements were made as described previously for the new K1 compositions $\text{La}_x\text{Pr}_{2-x}\text{NiO}_{4+d}$ ($x = 1.9, 1.2$ and 1.0) and the results for D_{chem} and k_{chem} are shown in Figure 4. For D_{chem} , the activation energies for each composition are similar. Much wider variations are observed in both the activation energy and magnitude of k_{chem} . $\text{La}_{1.9}\text{Pr}_{0.1}\text{NiO}_{4+\delta}$ has the highest value of k_{chem} but $\text{LaPrNiO}_{4+\delta}$ has both a high value of k_{chem} and a low activation energy. Further analysis of these data and more detailed comparison requires conversion of the chemical parameters to the self diffusion and exchange parameters. This conversion requires a knowledge of the variation of the stoichiometry with temperature and pO_2 and these experiments are in progress.

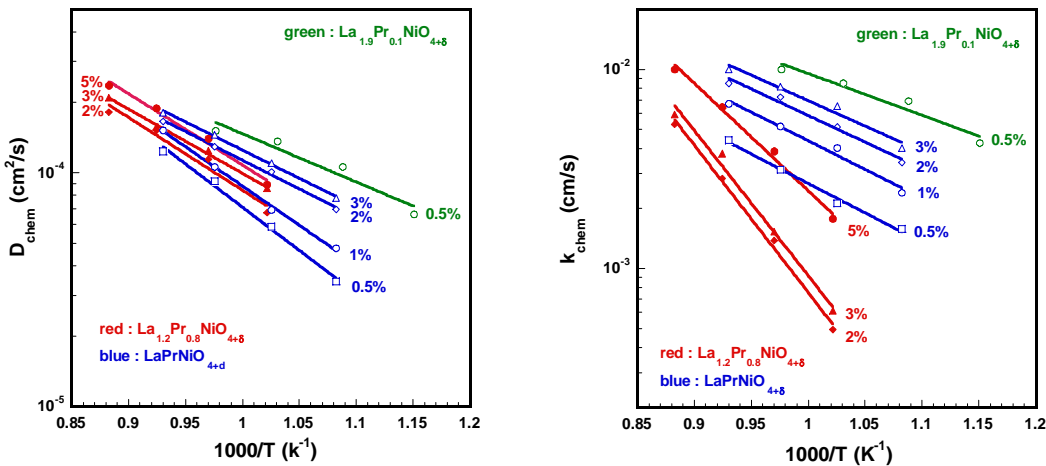


Figure 4 Values of D_{chem} (left) and k_{chem} (right) of $\text{La}_x\text{Pr}_{2-x}\text{NiO}_{4+\delta}$ ($x = 1.9, 1.2, 1$)

5. Combinatorial Approach to Measurement of Transport Parameters.

Perovskite and perovskite - related oxides are noteworthy for their tolerance of a very wide range of compositions. This is an advantage in that variations in composition can be used to simultaneously optimize several important properties such as surface exchange rate, diffusion coefficient, thermal expansion, and substrate reactivity. The disadvantage is that the matrix of possible compositions is very large and serial evaluation of properties is time consuming. Consequently, we have decided to adopt a combinatorial approach whereby many compositions can be screened for one or more properties using a single specimen. As a first step, we plan to investigate compositions in the $\text{LaFeO}_3 - \text{SrFeO}_{2.5}$ system which have been shown recently to be of interest as cathode materials for intermediate temperature operation. Eventually, we plan to expand the scope to include four different oxide components. We will use the two oxide component system to develop the technique and the processing conditions needed to prepare samples and the evaluation techniques. Samples will be prepared in the form of thin films by pulsed laser deposition (PLD) on single crystal yttria stabilized zirconia substrates. The general approach is shown in Figure 5.

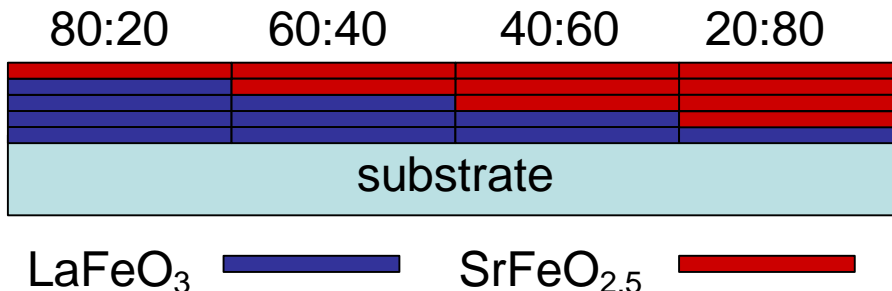


Figure 5. Schematic of the Approach to Make Multiple Compositions on One Substrate.

A shadow mask will be used to deposit the first oxide (LaFeO_3 in Figure 5) in steps of different thickness. In a second step, the second oxide ($\text{SrFeO}_{2.5}$ in Figure 5) will be

deposited in reverse order to produce a film of uniform total thickness. The films will be deposited with the substrate at ambient temperature where they will be amorphous.

To date, we have synthesized the targets, constructed the mask, and begun to determine the deposition parameters. The initial film synthesis to determine the crystallization temperatures has been completed (Task 5.1) and we have made the first measurements to study the interdiffusion.

5.1 Interdiffusion of Amorphous Bilayer Films of LaFeO_3 and $\text{SrFeO}_{2.5}$.

Our first goal is to make combinatorial thin films in the LaFeO_3 – $\text{SrFeO}_{2.5}$ system. This requires the interdiffusion of amorphous films of two separate compositions. In the last quarter, we concluded that, as a guideline the amorphous films should be annealed at temperatures lower than 400 °C for an appropriate period of time to interdiffuse the two compositions, and then annealed at temperatures higher than 650 °C to ensure the complete crystallization of the composite films. In this quarter, we made LaFeO_3 – $\text{SrFeO}_{2.5}$ two layer structures and annealed them using the above conditions.

Two types of amorphous films, LaFeO_3 on $\text{SrFeO}_{2.5}$ ($\text{LaFeO}_3/\text{SrFeO}_{3-d}$) and the reverse ($\text{SrFeO}_{3-d}/\text{LaFeO}_3$), were deposited on LaAlO_3 (LAO) substrates. The deposition method was the same as described in the previous report. The specific procedure used to treat the films was a two-step heat treatment in O_2 , first at 380°C for 110 h and then 715 °C for 8h.

XRD patterns of the annealed films are shown in Figures 1(a) and (b). The two large peaks (2θ at 24° and 48°) are from LAO substrate (001) and (002) diffraction lines. For $\text{SrFeO}_{3-d}/\text{LaFeO}_3$ film (Fig. 1(a)), the film peaks can be indexed as from the powder $\text{SrFeO}_{2.5}$ (17-0932), indicating that the film is not oriented. For $\text{LaFeO}_3/\text{SrFeO}_{3-d}$ film

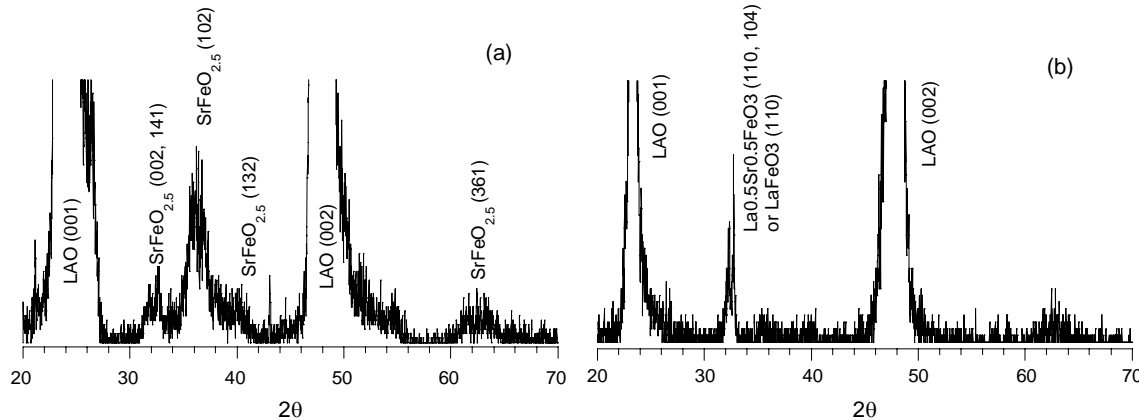


Figure 6. XRD spectra of annealed thin films on LAO substrate, a) $\text{SrFeO}_3/\text{LaFeO}_3$ b) $\text{LaFeO}_3/\text{SrFeO}_3$, after heated in O_2 at 380 °C for 110 h and followed by 715 °C for 8 h.

(Fig. 1(b)), we see only one peak, indicating that the film is oriented. The peak at 32.7° could be either from the LaFeO_3 (110) diffraction line (75-0439) or from $\text{La}_{0.5}\text{Sr}_{0.5}\text{FeO}_3$ (110) and (104) diffraction (82-1962). If it is the latter, the heat treatment succeeded in

interdiffusing the two compositions. The LaFeO_3 / SrFeO_3 sample was then further examined by SIMS to determine the extent of interdiffusion.

5.2 Surface Analysis of LaFeO_3 / SrFeO_3 on LAO

A survey scan was performed to determine the mass of the most intense elements sputtered from the two layer sample. Initially a negative ion scan was performed in the hope of increasing the sensitivity. The intensity of metal oxides in a negative ion scan is generally greater than in a positive ion scan. Charge build up, however, limits the sensitivity even with charge neutralization and mass 88 is obtained from Sr as well as from FeO_2 . Consequently, a positive Ga^+ survey scan was performed. In this case the mass of each element is selected. Interestingly LaO of mass 155 amu appears in the positive ion scan and was monitored also. Ga was also monitored to confirm the separation of the layers and to check for matrix effects. The masses monitored were ^{16}O , ^{27}Al , ^{69}Ga , ^{56}Fe , ^{88}Sr , ^{139}La , and $^{155}(\text{LaO})$.

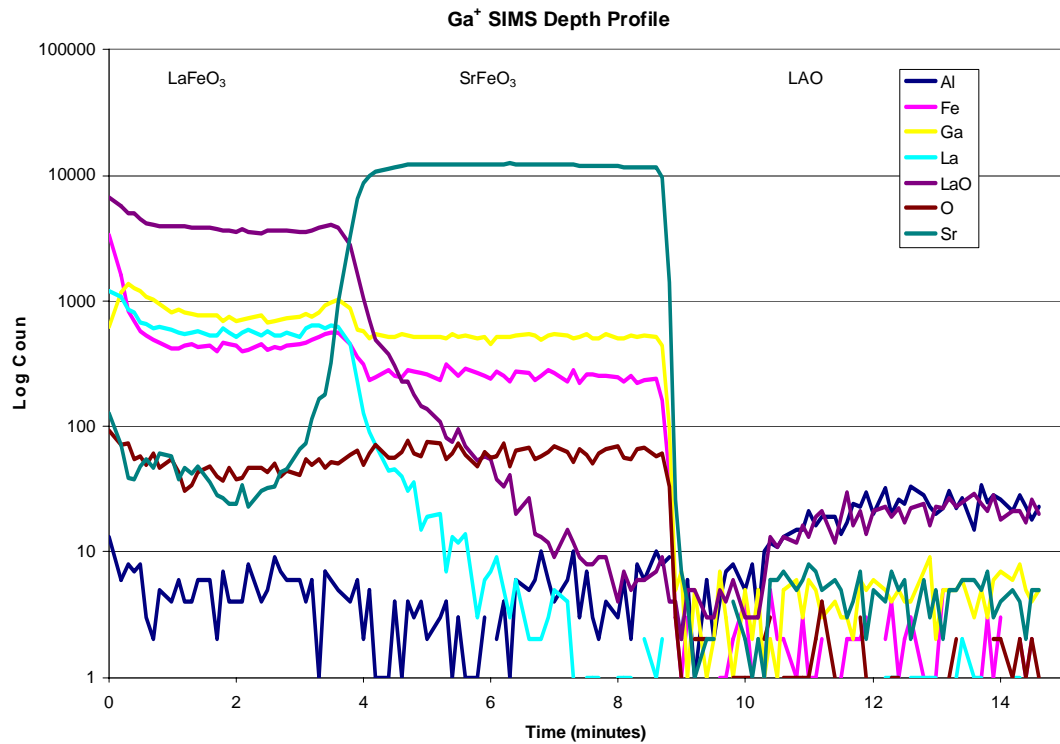


Figure 7 Ga^+ SIMS depth profile of LaFeO_3 on SrFeO_3 on a LAO substrate.

A Ga^+ depth profile was performed at 5000 times normal magnification at 60 deg to the sample normal at 25 kV incident energy with charge neutralization throughout. The depth profile is shown in Figure 7. From left to right, the LaFeO_3 top layer, the SrFeO_3 layer, and the lanthanum aluminate (LAO) substrate are observed. The Fe intensity and thus concentration appear constant in the first two layers, as expected from the stoichiometry. The Al intensity is very low and is also constant in the first two layers and is attributed to background noise indicating that Al diffusion is negligible. The Ga intensity in the first two layers is constant indicating that matrix effects are not of concern. In the first region,

the La intensity is high and then decreases to background noise in the second region indicating that the first layer is LaFeO_3 and that some La diffusion into the second layer has occurred. In the first region, the Sr intensity is low but is above the background noise level. The Sr intensity rises sharply to a high constant value in the second region. The second layer is SrFeO_{3-x} and Sr diffusion into the first layer occurs to a greater extent than the La diffusion in the reverse direction. The third region is indicated by an abrupt drop in intensity of all masses and is a result of the highly insulating nature of LAO.

Profilometer measurements do not give a crater depth from the depth profile because of the roughness of the sample surface. Thus, the sputter rates are not yet determined and the sputter depth is not known. Smooth single samples of each layer will be sputtered at the same magnification to determine these rates. The origin of the surface roughness will also be further investigated.

6. Conclusions

Single phase samples of $\text{La}_x\text{Pr}_{2-x}\text{NiO}_{4+d}$ ($x = 1.9, 1.2$ and 1.0) for comparison with the end members $\text{La}_2\text{NiO}_{4+x}$ and $\text{Pr}_2\text{NiO}_{4+x}$ have been prepared and characterized. Dense samples were prepared for conductivity and conductivity relaxation measurements. Conductivity measurements at different pO_2 values were measured for the samples and show significant variations with x . Conductivity relaxation measurements were made with different pressure switches. Thermogravimetric analysis measurements are in progress in order to determine the oxygen stoichiometry that is needed to extract the oxygen ion diffusion coefficients and the surface exchange coefficients for comparison with previous measurements. Amorphous two layer thin films of LaFeO_3 and $\text{SrFeO}_{2.5}$ have been prepared by PLD in amorphous form and their interdiffusion at 400°C investigated. Further work is necessary to find the optimum conditions and to reduce surface roughness that occurs during annealing.

7. References

1. *Electrochemical Intercalation of Oxygen in $\text{La}_2\text{NiO}_{4+x}$: Phase Separation Below Room Temperature*, Yazdi, I.; Bhavaraju, S.; DiCarlo, J. F.; Scarfe, D. P.; Jacobson, A. J., *Chem. Mater.* (1994) 6 2078-2084.
2. *Electrochemical Intercalation of Oxygen in $\text{Nd}_2\text{NiO}_{4+x}$ ($0 \leq x \leq 0.18$) at 298K*, Bhavaraju, S.; Di Carlo, J. F.; Scarfe, D. P.; Yazdi, I.; Jacobson, A. J., *Chem. Mater.* (1994) 6 2172-2176.
3. *Oxygen diffusion & surface exchange in $\text{La}_{2-x}\text{Sr}_x\text{NiO}_{4+x}$* , Skinner, S.J.; Kilner, J.A., *Solid State Ionics* (2000) 135 709-712.
4. *Oxygen diffusion and surface exchange in the mixed conducting perovskite $\text{La}_{0.6}\text{Sr}_{0.4}\text{Fe}_{0.8}\text{Co}_{0.2}\text{O}_{3-x}$* , Benson, S. J.; Chater, R.J.; Kilner, J. A. *Proc. Electrochem. Soc.* (1998) 1997-24 596-609.
5. *Ionic transport in oxygen-hyperstoichiometric phases with K_2NiF_4 -type structure*, Kharton, V. V.; Viskup, A. P.; Kovalevsky, A. V.; Naumovich, E. N.; Marques, F. M. B., *Solid State Ionics* (2001) 143 337-353.
6. *Transport and Permeation Properties of $\text{La}_2\text{NiO}_{4+x}$* , Tichy, R.S.; Huang, K. Q.; Goodenough, J. B.; *Proc. Electrochem. Soc.* (2001) 2000-32 171.

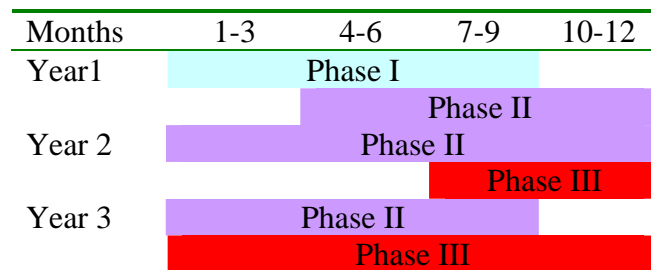
7. *Structure and properties of the Nickel (III) Oxide Family: $LnSr_5Ni_3O_{11}$* , James, M.; Attfield, J. P.; Rodriguez-Carvajal, J., *Chem. Mater.* (1995) 7 1448.
8. *Synthesis, Structure, and Properties of a Novel Metallic Nickel (III) Oxide, $CeSr_7Ni_4O_{15}$* , James, M.; Attfield, J. P., *Chem. Mater.* (1995) 7 2338.
9. *Nonstoichiometric K_2NiF_4 Type Phases in the Lanthanum Cobalt Oxygen System*, Lewandowski, J. T.; Beyerlein, R. A.; Longo, J. M.; McCauley, R. A., *J. Amer. Ceram. Soc.* (1986) 69 699-703.
10. *An Electrical Conductivity Relaxation Study of $La_{0.6}Sr_{0.4}Fe_{0.8}Co_{0.2}O_{3-x}$* , Wang, S.; van der Heide, P. A. W.; Chavez, C.; Jacobson, A. J.; Adler, S. B. *Solid State Ionics* (2003) 156 201-208.
11. *YSZ – Supported Cathodes of Rare Earth Nickelates Ln_2NiO_{4+x} For ITSOFC (650 °C)*, Bassat, J. M.; Boehm, E.; Grenier, J. C.; Mauvy, F.; Dordor, P.; Pouchard, M., *Fifth European Solid State Fuel Cell Forum*, (2002) 586-593.

8 List of Acronyms and Abbreviations

CGO	Cerium Gadolinium Oxide
ECR	Electrical Conductivity Relaxation
EPMA	Electron Probe MicroAnalysis
GDC	Gadolinia Doped Ceria (see CGO)
LSGM	Lanthanum Strontium Magnesium Gallate
PLD	Pulsed Laser Deposition
TGA	Thermogravimetric Analysis
YSZ	Yttria Stabilized Zirconia
IEDP	Isotope Exchange and Depth Profiling

9. Milestones and Scope of Work

The project is divided into three phases that will overlap as shown in the timelines below



Phase I: The Phase I objectives are to complete the characterization of a set of perovskite materials for which performance data already exists at PNNL. We will then measure the relevant kinetic parameters. The comparison the real performance data with the fundamental kinetic parameters will be used to guide materials selection in Phase II.

Phase II: The Phase II objectives of the project are to synthesize and characterize new cathode materials and to measure their kinetic parameters. The thermal and chemical compatibility with different electrolytes will be determined. Based on these results, a

subset of the best materials will be selected for single cell tests. Some additional compositions will be synthesized if indicated by the single cell test data.

Phase III: The phase three objectives are to evaluate the performance of the best materials identified in Phase I and II. The optimum electrode composition and microstructure will be determined and longer term performance characteristics evaluated.

Updated Milestones for Year 1

The updated milestones reflect two program adjustments since the original submission. The first is that we have started work on the K1 compositions ahead of the P1 compositions. The latter have been moved into the second half of the first year. The second is that in order to accelerate the thin film materials selection work we have decided to adopt a combinatorial approach which will permit the simultaneous synthesis of many compositions.

PHASE I

Task 1.0	Four modified perovskite oxide compositions (P1) selected by UH and PNNL will be synthesized and characterized by X-ray diffraction (XRD) and electron microprobe analysis (EMPA) (Months 6-9) in progress
Task 2.0	The chemical compatibility with YSZ, CGO and LSGM electrolytes will be determined (Months 6-9) in progress
Task 3.0	The temperature dependence of the dc conductivity and stoichiometry will be determined in air for the P1 compositions. (Months 6-9)
Task 4.0	The diffusion coefficients and surface exchange rates will be measured by electrical conductivity relaxation (Months 6-12)
Task 5.1	Thin films of perovskite compositions will be synthesized by PLD using a combinatorial approach. (Months 3-9) in progress
Task 5.2	Electrode-electrolyte interfaces will be characterized for thin films of cathode materials by AC impedance spectroscopy (Months 9-12)
Task 6.0	Electrode-electrolyte interfaces will be characterized for thin films of cathode materials by IEDP (9-12)

PHASE II

Task 1.0	Four modified perovskite oxide compositions (P2) will be synthesized and characterized by XRD and EMPA (Months 9-12)
Task 1.1	Two A_2BO_4 compositions (K1) will be synthesized and characterized by XRD and EMPA. (Months 1-4) completed
Task 1.2	Three additional A_2BO_4 compositions (K2) will be synthesized and characterized by XRD and EMPA. (Months 6-9) completed
Task 2.0	The chemical compatibility with YSZ, CGO and LSGM electrolytes will be determined for P2 (Month 12)
Task 2.1	The chemical compatibility with YSZ, CGO and LSGM electrolytes will be determined for K1 (Month 7) in progress
Task 2.2	The chemical compatibility with YSZ, CGO and LSGM electrolytes will be determined for K2 (Month 9)
Task 3.0	The dc conductivity and stoichiometry will be determined in air for the K1 compositions that have chemical compatibility. (Months 4-6) completed

Task 4.0 The diffusion coefficients and surface exchange rates will be measured by electrical conductivity relaxation for the **K1** materials evaluated in Task 3 (Months 6-12). **completed**

Task 4.1 K1 samples will be characterized in symmetric cells by AC impedance spectroscopy (Months 6-9) to confirm the measured values of k_{ex} .

Task 5.0 Electrode-electrolyte interfaces will be characterized for thin films of cathode materials selected from Task 4.0 by AC impedance spectroscopy (Months 10-33).

Task 6.0 Electrode-electrolyte interfaces will be characterized for thin films of cathode materials selected from Task 4.0 by IEDP (Months 10-33)

Task 7.0 Results from Tasks 4.0, 5.0, and 6.0 will be used as they become available to select cathode electrolyte combinations for single cell tests (Months 10-33).